JITK (JURNAL ILMU PENGETAHUAN DAN TEKNOLOGI KOMPUTER)

VOL. 12. NO. 1 AUGUST 2026
P-ISSN: 2685-8223 | E-ISSN: 2527-4864
DOI: 10.33480/jitk.v12i1.7963

EFFICIENT MRI-BASED BRAIN TUMOR CLASSIFICATION USING PRUNED SQUEEZENET ARCHITECTURE

Ade Ismiaty Ramadhona Ht. Barat[1*]; Poningsih[1]; Anjar Wanto[1]

Informatics Study Program[1]
STIKOM Tunas Bangsa, Pematangsiantar, Indonesia[1]
www.stikomtunasbangsa.ac.id[1]
ade@amiktunasbangsa.ac.id*, poningsih@amiktunasbangsa.ac.id, anjarwanto@amiktunasbangsa.ac.id

(*) Corresponding Author
(Responsible for the Quality of Paper Content)

Abstract—*Brain tumors are among the most serious neurological diseases, requiring accurate diagnosis to support effective treatment. Magnetic Resonance Imaging (MRI) is widely used for brain tumor detection because it provides detailed visualization of brain structures. However, manual MRI interpretation is time-consuming and highly dependent on radiologists' expertise, potentially leading to inconsistent diagnoses. This study evaluates the performance of several deep learning architectures, including VGG16, DenseNet121, Custom CNN, and SqueezeNet, for multiclass brain tumor classification using MRI images. To address the computational limitations of deep neural networks in resource-constrained medical environments, a structured pruning approach based on polynomial decay sparsity scheduling was applied to the SqueezeNet model to reduce model complexity while preserving predictive performance. Experiments were conducted on a multiclass MRI dataset consisting of glioma, meningioma, pituitary tumor, and non-tumor images. The proposed pruned SqueezeNet achieved a classification accuracy of 98.70% and an AUC of 0.998, while reducing the model size to 2,970 KB and achieving an inference time of 105.40 ms. These results demonstrate that structured pruning effectively improves computational efficiency without significantly compromising classification accuracy, making the model suitable for deployment in resource-limited medical settings. Nevertheless, further validation using larger and multi-institutional MRI datasets is required before clinical implementation.*

Keywords: *Brain Tumor Classification, Model Compression, MRI, Pruning, SqueezeNet.*

Intisari—*Tumor otak merupakan salah satu penyakit neurologis yang memerlukan diagnosis akurat untuk mendukung penentuan terapi. Magnetic Resonance Imaging (MRI) menjadi modalitas utama dalam mendeteksi tumor otak karena mampu memberikan visualisasi struktur otak secara rinci. Namun, analisis citra MRI secara manual memerlukan waktu yang relatif lama dan sangat bergantung pada pengalaman radiolog sehingga berpotensi menimbulkan variasi hasil diagnosis. Penelitian ini mengevaluasi kinerja beberapa arsitektur deep learning, yaitu VGG16, DenseNet121, Custom CNN, dan SqueezeNet, untuk klasifikasi multiclass tumor otak berbasis citra MRI. Untuk mengatasi tingginya kompleksitas komputasi model deep learning, penelitian ini menerapkan pendekatan structured pruning pada arsitektur SqueezeNet menggunakan polynomial decay sparsity scheduling guna mengurangi kompleksitas model tanpa menurunkan performa klasifikasi secara signifikan. Pengujian dilakukan menggunakan dataset MRI yang terdiri atas empat kelas, yaitu glioma, meningioma, pituitary tumor, dan non-tumor. Hasil eksperimen menunjukkan bahwa model SqueezeNet hasil pruning mencapai akurasi 98,70% dengan nilai AUC 0,998, mampu mengurangi ukuran model menjadi 2.970 KB, serta menghasilkan waktu inferensi 105,40 ms. Hasil tersebut menunjukkan bahwa structured pruning efektif meningkatkan efisiensi komputasi dengan tetap mempertahankan akurasi klasifikasi yang tinggi sehingga berpotensi diterapkan pada lingkungan medis dengan keterbatasan sumber daya komputasi. Meskipun demikian, validasi lebih lanjut menggunakan dataset*

MRI yang lebih besar dan berasal dari berbagai institusi masih diperlukan sebelum model dapat diimplementasikan pada lingkungan klinis.

Kata Kunci*: Klasifikasi Tumor Otak, Model Kompresi, MRI, Pruning, SqueezeNet.*

INTRODUCTION

The human brain is a highly sophisticated organ that plays a central role in regulating cognition, sensory processing, and motor functions [1], [2]. Any abnormality affecting brain tissue can severely interfere with neurological activity and pose serious risks to overall health [3]. Among various neurological disorders, brain tumors are considered particularly dangerous because they can disrupt normal brain operations and negatively affect patient survival [4]. Brain tumors may develop from abnormal cell growth within the brain itself or from metastatic cancer cells spreading from other body regions [5], [6].

In medical imaging studies, brain tumors are commonly classified into three major categories: glioma, meningioma, and pituitary tumors, while healthy brain MRI images are typically categorized as a separate class for automated classification systems [7], [8]. Alongside these tumor categories, normal brain images are typically classified as a distinct category (notumor) to facilitate automated classification activities [9]. Accurate and timely identification of these tumor types is crucial for supporting appropriate treatment planning and improving patient prognosis.

Magnetic Resonance Imaging (MRI) is widely recognized as one of the most effective imaging techniques for diagnosing brain tumors because it can produce detailed visualizations of soft tissues and internal brain structures [10], [11]. MRI scans enable clinicians to examine tumor position, morphology, and structural abnormalities with high precision [12].

However, manual interpretation of MRI data remains a difficult and time-intensive task that strongly depends on the expertise of radiologists and medical specialists [13], [14]. In addition, variations in human assessment may lead to inconsistent diagnoses, especially when dealing with large-scale imaging datasets. Therefore, artificial intelligence–based computer-aided diagnostic systems have become increasingly important for supporting automated brain tumor detection and classification [15], [16], [17], [18].

In recent years, artificial intelligence approaches, especially deep learning techniques such as Convolutional Neural Networks (CNNs), have shown significant progress in the field of medical image analysis [19], [20], [21]. Several pretrained CNN architectures, including VGG16, DenseNet, and EfficientNet, have achieved strong performance in brain tumor classification studies, frequently reporting accuracy values above 94% [22]. Despite their high predictive capability, these models generally contain large numbers of parameters and require substantial computational resources. Such characteristics often increase memory consumption and inference time, limiting their applicability in real-time clinical environments and resource-limited healthcare systems.

To overcome these computational limitations, many studies have explored lightweight CNN architectures and architecture optimization strategies. Lightweight models such as SqueezeNet are capable of providing competitive classification performance while using significantly fewer parameters compared with conventional deep CNN models. For example [23], the LeaSE neural architecture search successfully generated efficient network configurations tailored to brain tumor classification It reached a test accuracy of 90.6% while requiring substantially fewer parameters than conventional deep models, including ResNet101, thereby demonstrating improved efficiency without sacrificing performance. While these methods demonstrate the potential of automated architecture optimization. The search process itself often demands extensive computational resources, which restricts its feasibility in practical medical applications.

A study demonstrates that integrating wavelet transform techniques with deep learning models can improve the classification performance of brain tumor MRI images [24]. By applying multiple wavelet-based preprocessing approaches, the framework was able to capture more detailed image characteristics before feature extraction using convolutional neural networks and vision transformer architectures. Experimental results showed that the ensemble-based approach combining MobileNet-v3, Vision Transformer, ResNeXt, and DenseNet-201 achieved the highest classification accuracy of 85.03%, outperforming individual model configurations.

VOL. 12. NO. 1 AUGUST 2026
P-ISSN: 2685-8223 | E-ISSN: 2527-4864
DOI: 10.33480/jitk.v12i1.7963

Another line of research focuses on combining deep learning models with advanced optimization strategies [25], Hybrid frameworks that integrate preprocessing, segmentation, and optimization algorithms have been introduced to enhance classification accuracy. For example, the EWHO-SqueezeNet framework combines denoising, ROI extraction, segmentation with M-SegNet, and classification using SqueezeNet optimized via an evolutionary algorithm. Although such multi-stage pipelines can improve classification accuracy, they also introduce additional computational complexity and may reduce inference efficiency, which is a critical factor for clinical deployment.

Model compression techniques such as pruning have also gained increasing attention as effective strategies for reducing the computational cost of deep neural networks [26]. Although SqueezeNet was originally designed as a compact CNN architecture and achieved 90% accuracy, further optimization is still important for deployment in practical medical imaging applications, particularly in edge-based healthcare systems and environments with limited computational resources [27], [28], [29]. Most lightweight CNN studies mainly concentrate on simplifying network architecture, whereas limited research has investigated the impact of structured pruning on already compact architectures for multiclass brain tumor MRI classification [30], [31]. In addition, prior pruning studies rarely examine the balance between computational efficiency and predictive performance in highly parameter-efficient models such as SqueezeNet [32]. Consequently, the effectiveness of applying structured pruning to further compress lightweight CNNs while maintaining reliable diagnostic performance remains insufficiently explored [33], [34].

Based on these challenges, this study proposes a structured pruning strategy integrated with polynomial decay sparsity scheduling for SqueezeNet in multiclass brain tumor MRI classification tasks [35], [36]. The proposed approach gradually removes less important parameters while preserving essential feature representations required for accurate tumor recognition. Instead of emphasizing classification accuracy alone, this research focuses on achieving an effective balance between predictive capability and computational efficiency to support practical deployment in medical imaging systems.

The main contributions of this study can be summarized as follows. First, this research explores the application of structured pruning integrated with polynomial decay sparsity scheduling on the lightweight SqueezeNet model for multiclass brain tumor MRI classification. Second, the proposed approach analyzes the balance between model efficiency and predictive capability by decreasing computational complexity, parameter size, and inference time while preserving competitive classification performance. Third, comparative experiments involving DenseNet121, VGG16, and Custom CNN demonstrate that the pruned SqueezeNet architecture can serve as an efficient solution for medical image classification in environments with limited computational resources.

MATERIALS AND METHODS

The methodology applied for developing an efficient deep learning framework for multiclass brain tumor classification using MRI images is explained in this section.

Data Collection

This study employs a publicly available brain MRI dataset obtained from Kaggle, consisting of 7,023 labeled images categorized into four classes: glioma, meningioma, pituitary, and notumor. The dataset includes 5,712 images for training and 1,311 images for testing. In terms of class distribution, the dataset is slightly imbalanced, where the notumor category contains a relatively higher number of samples compared to the tumor classes.

Data Preprocessing

MRI images were rescaled to a resolution of 224 × 224 pixels and normalized within an intensity range of 0–1 to support stable training and improve convergence performance. To increase model generalization capability and minimize overfitting, several data augmentation methods were implemented during training, including random rotation, horizontal flipping, zoom transformation, and spatial shifting, while maintaining the original class balance of the dataset. The overall dataset distribution is presented in Table 1.

Table 1. Number of Images

No	Class Category	Number of Images
1	glioma	1,621
2	meningioma	1,645
3	pituitary	1,757
4	notumor	2,000
	Total Images	7,023

Source: (Research Result, 2026)

Table 1 displays the dataset utilised in this research, obtained from Kaggle (https://www.kaggle.com/datasets/masoudnickparvar/brain-tumor-mri-dataset), consisting of four categories. Figure 1 presents sample MRI scans corresponding to the four classes of brain tumors.

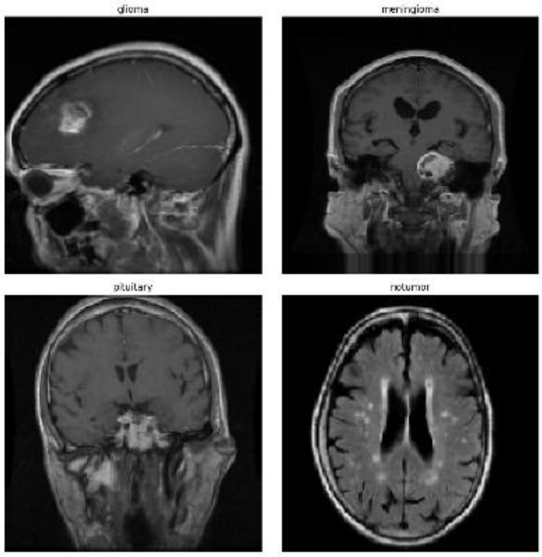

Source: (Research Result, 2026)
Figure 1. Sample of Brain Tumors MRI Images

Figure 1 presents representative MRI images from the four classification categories examined in this study: glioma, meningioma, pituitary, and notumor. The samples illustrate the visual complexity and structural variability among tumor classes, highlighting the importance of deep learning approaches capable of capturing fine-grained image characteristics [37]. These examples provide visual context for the classification task by illustrating the distinct structural traits associated with each tumor type. The illustration highlights the inherent challenges of categorizing brain tumors from MRI scans, reinforcing the importance of sophisticated deep learning approaches that can capture fine-grained visual distinctions among tumor types. These samples offer visual context for the categorization challenge by demonstrating the unique anatomical characteristics linked to each tumor type. By illustrating representative MRI images, this visual representation demonstrates the complex nature of brain tumor classification and stresses the necessity for advanced deep learning frameworks capable of identifying fine-grained visual variations among different tumor categories.

The preprocessing pipeline was designed to ensure that the MRI inputs were adequately cleaned, balanced, and optimized for efficient model training [38]. Although the dataset exhibits mild class imbalance, particularly in the notumor category, the class distribution remains sufficiently representative for multiclass classification experiments. To enhance generalization and mitigate overfitting risks due to limited sample size, the training set was augmented using random rotations, horizontal flips, zoom transformations, and spatial shifts thereby increasing data variability and improving model robustness.

Research Stages

This study aims to develop an efficient deep learning framework for brain tumor classification using MRI images based on a pruned SqueezeNet architecture. The proposed method focuses on reducing model complexity, parameter size, and inference time while maintaining competitive classification performance, making it appropriate for deployment in resource-constrained environments. Each stage of the research process was systematically designed in accordance with established deep learning practices. Figure 2 presents the overall workflow of the proposed methodology.

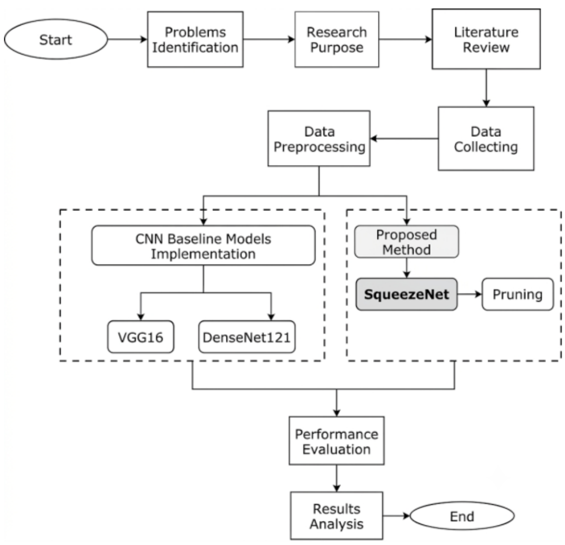

Source: (Research Results, 2026)
Figure 2. Research Workflow

The research workflow implemented in this study is illustrated in Figure 2, delineating the principal stages:

Accredited Rank 2 (Sinta 2) based on the Decree of the Dirjen Penguatan RisBang Kemenristekdikti No.225/E/KPT/2022, December 07, 2022. Published by LPPM Universitas Nusa Mandiri

VOL. 12. NO. 1 AUGUST 2026
P-ISSN: 2685-8223 | E-ISSN: 2527-4864
DOI: 10.33480/jitk.v12i1.7963

1. Problem Identification
   The study approach starts by figuring out what the biggest problems are with MRI-based brain tumor categorization. One of these problems is the necessity for accurate diagnosis while making the procedure less complicated so that clinical decision-making can be done quickly and easily.

2. Research Purpose
   This study aims to improve brain tumor classification performance while reducing model complexity by applying pruning techniques to the SqueezeNet architecture, addressing the observed limitations.

3. Literature Review
   This paper examines recent advancements in MRI-based brain tumor classification, lightweight CNN architectures, and pruning algorithms to highlight research deficiencies and lay the groundwork for the suggested methodology.

4. Data Collection
   To make sure that the study is diverse and can be repeated, MRI brain tumor datasets are taken from publicly available sources.

5. Data Preprocessing
   To increase picture quality and model generalization, the gathered MRI images are preprocessed by resizing, normalizing, and adding more data.

6. CNN Baseline Models Implementation
   Baseline CNN models, notably custom CNN, VGG16 and DenseNet121, are grounded in the findings of reference[22], which highlight the strong classification accuracy achievable with MRI brain tumor images.

7. Proposed Method
   The proposed method integrates SqueezeNet with structured pruning based on polynomial decay. This approach reduces parameters and computational requirements while preserving classification accuracy, hence improving efficiency and making the model suitable for deployment in resource-constrained environments.

8. Performance Evaluation
   The model's efficacy was assessed by a confusion matrix and standard classification measures, encompassing precision, recall, F1-score, total accuracy, and AUC. Additionally, model size (in kilobytes) and inference time (in milliseconds) were assessed to ascertain deployment feasibility, particularly for real-time medical applications.

9. Result Analysis.
   The Pruned SqueezeNet attained accuracy similar to baseline CNNs while reducing model complexity and inference cost and processing requirements. These findings confirm the efficacy of pruning in enhancing both performance and efficiency, underscoring the model's capability for real-time brain tumor classification in resource-limited settings.

Convolutional Neural Network Models

Convolutional Neural Networks (CNNs) represent a class of deep learning architectures that are widely applied in image classification tasks because of their ability to automatically learn hierarchical representations from raw image inputs. In medical image analysis, CNN models have shown strong capability in interpreting MRI scans by recognizing spatial and texture-related patterns that are important for disease identification. A conventional CNN architecture generally consists of convolutional layers for extracting features, pooling layers for reducing feature dimensions, and fully connected layers for classification, enabling the model to learn discriminative features automatically without manual feature engineering [39]. CNN-based techniques have been extensively implemented for automated brain tumor MRI classification because they can directly capture discriminative spatial information from medical imaging datasets. To maintain consistency and reproducibility throughout the experiments, all evaluated architectures were trained and tested using the same hardware specifications and optimization configurations. The experimental environment utilized an Intel Core i3 11th Generation processor, Intel UHD Graphics, 8 GB RAM, and the Windows 11 operating system.

The evaluation process employed several assessment metrics, including accuracy, precision, recall, F1-score, AUC, confusion matrix, model size, and inference time, to obtain a comprehensive evaluation of predictive performance and computational efficiency. The assessment framework was not solely focused on classification accuracy but was also intended to investigate the balance between model compactness, inference speed, and predictive performance among the evaluated CNN architectures.

Baseline CNN Models

This study developed several baseline convolutional neural network models to provide a fair and consistent performance evaluation framework. DenseNet121, VGG16, and Custom CNN were selected as representative architectures based on prior studies that demonstrated their effectiveness in MRI-based brain tumor classification. These architectures are widely adopted in medical image analysis because of their ability to learn deep and discriminative representations from complex visual data. The baseline architectures shown in Figure 3.

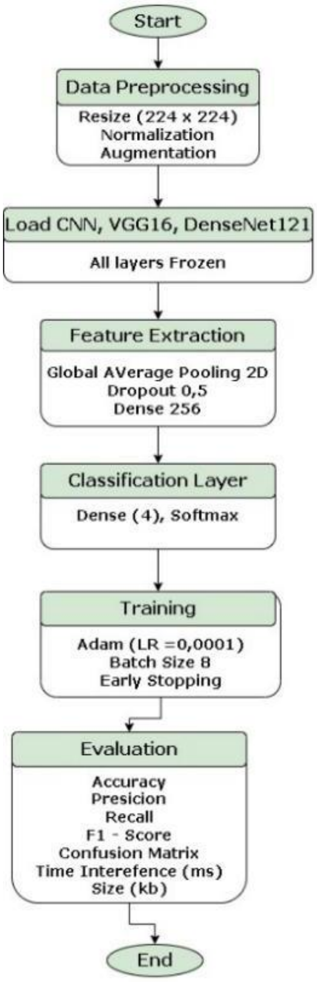

Source: (Research Results, 2026)
Figure 3. Baseline CNN Models

Figure 3 illustrates the overall workflow of the proposed brain tumor MRI classification framework based on convolutional neural network architectures and transfer learning methods. The framework consists of several stages, including data preprocessing, feature extraction, model training, classification, structured pruning, and performance evaluation. Pretrained architectures such as VGG16 and DenseNet121 were utilized alongside a Custom CNN model and SqueezeNet to investigate the effectiveness of different CNN-based approaches for multiclass brain tumor classification. In addition, structured pruning with polynomial decay sparsity scheduling was applied to the SqueezeNet architecture to reduce model complexity and improve inference efficiency while preserving classification capability.

Performance evaluation was conducted using several metrics, including accuracy, precision, recall, F1-score, AUC, confusion matrix, model size, parameter reduction, and inference time, to provide a comprehensive assessment of both predictive performance and computational efficiency. The evaluation framework was designed not only to measure classification capability but also to analyze the trade-off between model complexity, model compression, and inference efficiency across different CNN architectures in multiclass brain tumor MRI classification tasks.

Proposed Method

This study assesses the efficacy of the suggested Pruned SqueezeNet model. Structured pruning was utilized to enhance the architecture, achieving a balance between accuracy and efficiency. In comparable trials, the pruned SqueezeNet attained competitive classification performance while significantly decreasing model size and inference duration. These enhancements render the model especially appropriate for real-time brain tumor detection in resource-limited clinical settings.

To maintain a fair comparison among all models, identical experimental configurations were implemented throughout the training process. Each model used an input image size of 224 × 224 pixels, a batch size of 8, the Adam optimizer with a learning rate of 0.0001, and the categorical cross-entropy loss function. The same augmentation techniques were also applied to all architectures, including random rotation, width and height shifting, shear augmentation, zoom transformation, and horizontal flipping, with the objective of enhancing model generalization and minimizing overfitting.

For multiclass brain tumor classification adaptation, the pretrained models were modified by adding a customized classification head consisting of a Global Average Pooling layer, a

VOL. 12. NO. 1 AUGUST 2026
P-ISSN: 2685-8223 | E-ISSN: 2527-4864
DOI: 10.33480/jitk.v12i1.7963

dense layer containing 256 neurons with ReLU activation, a dropout layer with a dropout rate of 0.5 to improve regularization, and a final softmax layer producing four output categories. In addition, early stopping was incorporated during training to avoid excessive optimization once convergence had stabilized. Although the number of maximum epochs differed between the baseline and the proposed approach, the optimization strategy and evaluation procedure were consistently maintained across all experimental scenarios.

A comparison between the baseline models and the proposed methodology is illustrated in Figure 4.

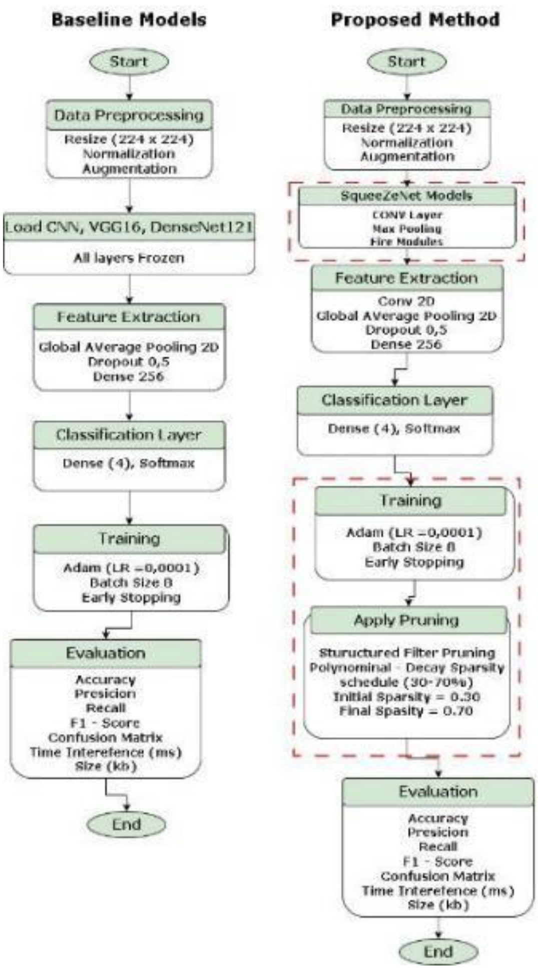

Source: (Research Results, 2026)

Figure 4. Comparison of Baseline Models and Proposed Method

Figure 4 presents the comparative framework used for brain tumor classification. The baseline architecture includes Custom CNN, VGG16, and DenseNet121 models, where convolutional layers were employed to extract image features, followed by pooling layers, dropout regularization, and dense layers for classification.

Pruning Configuration

To improve computational efficiency while maintaining predictive capability, structured pruning was applied to the SqueezeNet architecture using the TensorFlow Model Optimization Toolkit (TF-MOT). The pruning process progressively removed less important parameters during training using a polynomial decay sparsity schedule.

Structured pruning was applied to convolutional layers within the Fire modules of SqueezeNet, while the final classification layer was excluded to preserve output stability during multiclass prediction. Filter importance was determined using weight magnitude–based evaluation, where parameters with smaller magnitudes were considered less significant and gradually suppressed during training [40].

The sparsity level was controlled using a polynomial decay schedule formulated as follows:

$$s_t = s_f + s_i - s_f)\left(1 - \frac{t-t_0}{n-\Delta t}\right)^3 \quad (1)$$

Where (s_t) represents the sparsity level at training step (t), (s_i) denotes the initial sparsity, and (s_f) represents the target sparsity level. In this study, the pruning schedule was configured with an initial sparsity of 0.30 and a final sparsity of 0.70. The pruning process started from the beginning of training ((begin_step = 0)) and gradually increased until the final training step defined by the total number of training iterations.

During training, pruning was implemented using binary masking mechanisms provided by TF-MOT to suppress less important parameters while maintaining the original network structure. After training completion, the pruning wrappers were removed to generate the compressed model used for evaluation and inference. The pruning configuration employed in this study is summarized in Table 2.

Table 2. Pruning Configuration

Parameter	Value
Pruning Method	Polynomial Decay
Initial Sparsity	0.30
Final Sparsity	0.70
Begin Step	0
End Step	Total Training Step
Framework	TensorFlow Model Optimization Toolkit (TF – MOT)

Source: (Research Results, 2026)

VOL. 12. NO. 1 AUGUST 2026
P-ISSN: 2685-8223 | E-ISSN: 2527-4864
DOI: 10.33480/jitk.v12i1.7963

The proposed pruning strategy as shown in Table 2 was designed to reduce computational complexity and model size while maintaining competitive classification performance for multiclass brain tumor MRI classification.

RESULTS AND DISCUSSION

This section delineates the experimental assessment of diverse CNN designs, encompassing custom CNN, VGG16, DenseNet121, the SqueezeNet baseline, and the Pruned SqueezeNet, for multiclass brain tumor classification. Performance was assessed by training behavior and classification metrics to ascertain accuracy and stability. A comparative investigation indicates that structured pruning improves computational efficiency and generalization while preserving accuracy similar to that of bigger CNNs.

The optimized SqueezeNet significantly reduces model size and inference time, underscoring its suitability for real-time medical image processing in resource-limited settings.

Image Data Pre-Processing Results

The dataset utilized in this research was obtained from a publicly accessible Kaggle repository containing brain MRI images divided into four categories: glioma, meningioma, pituitary, and notumor. Predefined training and testing partitions were adopted to maintain consistency with prior benchmark studies. Table 3 summarizes the distribution of images within each subset, providing an overview of the dataset composition prior to the model development stage.

Table 3. Brain Tumor MRI Images Data Distribution

No	Class Category	Training Set	Testing Set	Total Images per Class
1	Glioma	1,321	300	1,621
2	Meningioma	1,339	306	1,645
3	Pituitary	1,457	300	1,757
4	NoTumor	1,595	405	2,000
	Total Images	5,712	1,311	7,023

Source: (Research Results, 2026)

Table 3 illustrates the allocation of MRI images across the four classification categories: glioma, meningioma, pituitary, and notumor. In total, the dataset consists of 7,023 images, including 5,712 training samples and 1,311 testing samples. Although the dataset distribution is generally balanced, the notumor category contains a slightly larger number of samples compared to the tumor categories, indicating the presence of minor class imbalance.

To minimize the impact of class imbalance on performance interpretation, the evaluation framework incorporated multiple assessment metrics, including precision, recall, F1-score, confusion matrix, and AUC scores. These metrics were selected to provide a more comprehensive evaluation of classification performance across all categories rather than depending exclusively on overall accuracy.

Image Data Classification Result

This section presents the results of multiclass brain tumor classification using Custom CNN, VGG16, DenseNet121, and the pruned SqueezeNet model. The discussion includes training performance, quantitative evaluation metrics, and comparative analysis among the evaluated architectures, with particular emphasis on the contribution of structured pruning in enhancing model efficiency, reducing inference time, improving generalization capability, and maintaining competitive classification performance.

Loss and Accuracy Curve

The loss and accuracy curves illustrate the training behavior of the Custom CNN, VGG16, DenseNet121, baseline SqueezeNet, and pruned SqueezeNet models. Across all evaluated architectures, both training and validation loss gradually decreased over successive epochs, while classification accuracy consistently improved during the optimization process. To ensure a fair comparison, all baseline models were trained using identical experimental settings. Figure 5 presents the training history of the baseline architectures.

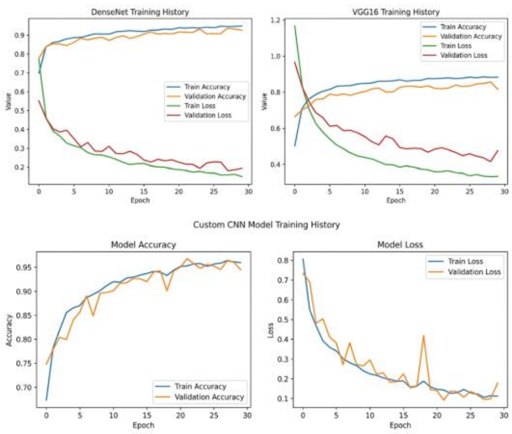

Source: (Research Results, 2026)

Figure 5. Baseline Models Loss And Accuracy Curve

VOL. 12. NO. 1 AUGUST 2026
P-ISSN: 2685-8223 | E-ISSN: 2527-4864
DOI: 10.33480/jitk.v12i1.7963

Figure 5 illustrates the training and validation performance of the baseline CNN architectures, including VGG16, DenseNet121, and Custom CNN, for multiclass brain tumor MRI classification. The training curves show that VGG16 and DenseNet121 achieved relatively stable convergence patterns with consistent validation performance. In contrast, the Custom CNN model demonstrated greater fluctuations during training, indicating higher sensitivity to dataset variability and limitations in feature generalization capability. These convergence behaviors serve as an experimental reference for comparison with the proposed pruned SqueezeNet framework shown in Figure 6.

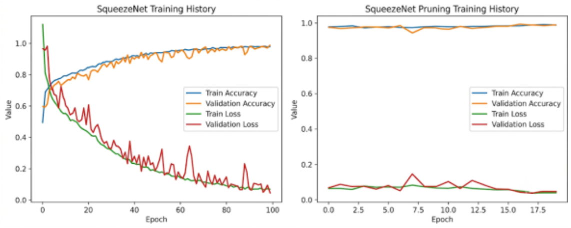

Source: (Research Results, 2026)

Figure 6. Proposed Method Loss And Accuracy Curve

Figure 6 presents the architecture and training behavior of the proposed SqueezeNet-based framework. The model integrates convolutional layers and Fire modules, followed by global average pooling and a classification layer for multiclass brain tumor recognition. To enhance computational efficiency, structured pruning combined with a polynomial decay sparsity schedule was implemented to progressively eliminate less important parameters during the optimization process.

The training curves indicate that the pruned SqueezeNet model preserved stable convergence behavior and competitive predictive capability while simultaneously reducing model complexity. Compared with the baseline architecture, the pruning strategy minimized parameter redundancy, reduced inference time, and lowered memory consumption without significantly decreasing classification performance. These observations indicate that structured pruning can improve computational efficiency while maintaining reliable predictive performance in lightweight CNN-based medical image classification tasks.

Confusion Matrix

The confusion matrix provides detailed insight into the classification performance of the baseline architectures by highlighting both correct predictions and misclassification patterns. Figure 7 presents the classification results on the testing dataset across the four categories: glioma, meningioma, pituitary, and notumor offering a comprehensive overview of prediction accuracy and error distribution among the evaluated models.

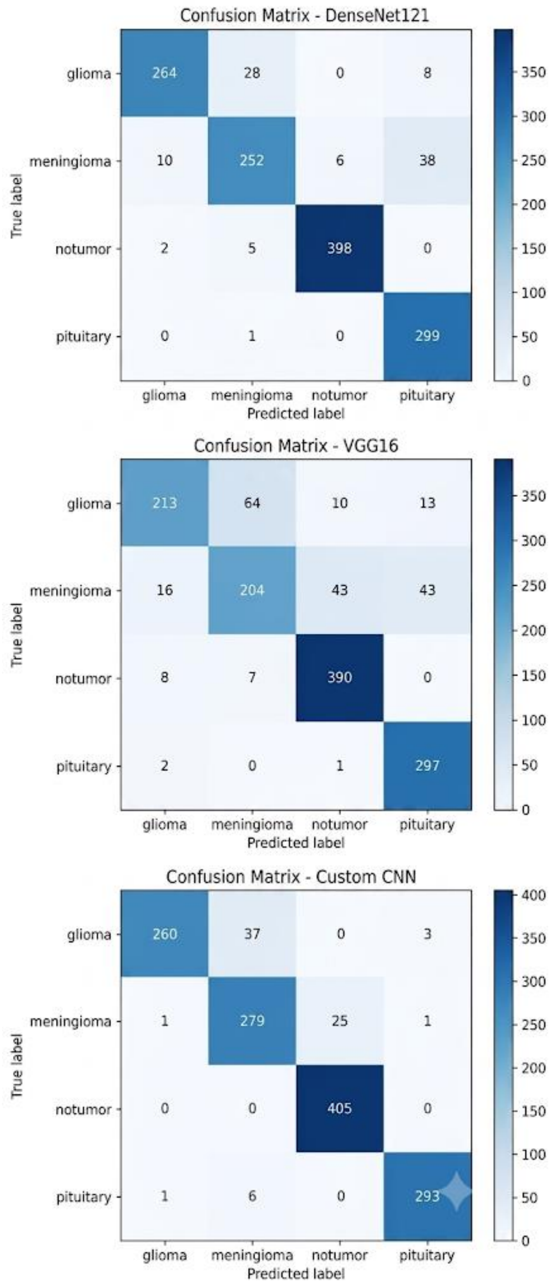

Source: (Research Results, 2026)

Figure 7. Baseline Models Confusion Matrix

Figure 7 presents the confusion matrices of baseline models, DenseNet121 shows high classification accuracy, with minimal misclassification across all classes. Glioma and Meningioma predictions are slightly confused with each other, while pituitary and notumor classes are identified with near-perfect precision. VGG16 exhibits intermediate efficacy, with significant misclassifications occurring between Glioma and Meningioma, as well as substantial overlap in predictions between meningioma and notumor cases. The custom CNN attains impressive outcomes, especially in the no-tumor category, which is categorized with flawless accuracy. Minor confusion is observed between glioma and meningioma, and a few pituitary cases are misclassified.

These matrices provide a complete insight of each model's strengths and limits in differentiating tumor types, enabling a platform for evaluating the improvements made by the proposed Pruned SqueezeNet as shown in Figure 8.

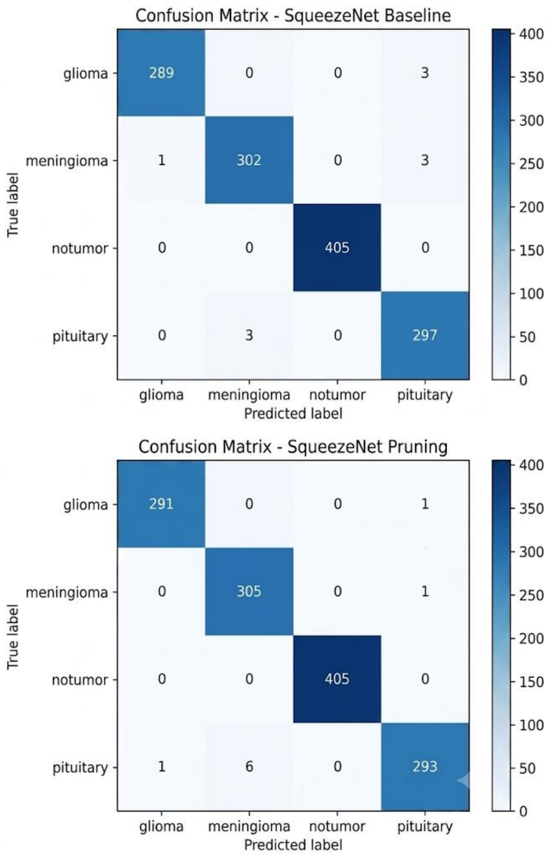

Source: (Research Results, 2026)
Figure 8. Proposed Method Confusion Matrix

Figure 8 presents the confusion matrix analysis of the suggested method, contrasting the baseline SqueezeNet with its pruned counterpart, both evaluated on the brain tumor classification task. In the baseline SqueezeNet, the glioma and meningioma categories exhibit minimal misclassifications, with many glioma instances incorrectly identified as meningioma or pituitary. The notumor and pituitary groups are classified with excellent accuracy, demonstrating significant separability in those classifications. The Pruned model achieves flawless classification for the no-tumor category and exhibits very slight misunderstanding in Pituitary predictions.

These results suggest that pruning not only reduces model complexity but also enhances generalization, as evidenced by the tighter prediction alignment across all tumor classes. The classification of findings encompasses the predictive effectiveness of all evaluated models via precision, recall, F1-score, and overall accuracy. Figure 9 presents the Classification Report for Baseline Models.

DenseNet121 Classification Report

	precision	recall	f1-score	support
glioma	0.96	0.88	0.92	300
meningioma	0.88	0.82	0.85	306
notumor	0.99	0.98	0.98	405
pituitary	0.87	1.00	0.93	300
accuracy			0.93	1311
macro avg	0.92	0.92	0.92	1311
weighted avg	0.93	0.93	0.92	1311

VGG16 Classification Report

	precision	recall	f1-score	support
glioma	0.89	0.71	0.79	300
meningioma	0.74	0.67	0.70	306
notumor	0.88	0.96	0.92	405
pituitary	0.84	0.99	0.91	300
accuracy			0.84	1311
macro avg	0.84	0.83	0.83	1311
weighted avg	0.84	0.84	0.84	1311

Custom CNN Classification Report

	precision	recall	f1-score	support
glioma	0.99	0.87	0.93	300
meningioma	0.87	0.91	0.89	306
notumor	0.94	1.00	0.97	405
pituitary	0.99	0.98	0.98	300
accuracy			0.94	1311
macro avg	0.95	0.94	0.94	1311
weighted avg	0.95	0.94	0.94	1311

Source: (Research Results, 2026)
Figure 9. Baseline Models Classification Report

Figure 9 displays the baseline classification reports, encapsulating precision, recall, and F1-score across four categories: glioma, meningioma, pituitary, and notumor. DenseNet121 and the custom CNN attained high accuracy, with the CNN demonstrating enhanced

VOL. 12. NO. 1 AUGUST 2026
P-ISSN: 2685-8223 | E-ISSN: 2527-4864
DOI: 10.33480/jitk.v12i1.7963

precision across categories. VGG16 exhibited diminished recall and F1-scores, especially for glioma and meningioma, indicating decreased sensitivity in identifying these tumor forms. Figure 10 displays the classification report for the proposed Pruned SqueezeNet.

SqueezeNet Baseline Classificatin Report

```
              precision    recall  f1-score   support

      glioma       1.00      0.96      0.98       300
  meningioma       0.96      0.99      0.98       306
     notumor       1.00      1.00      1.00       405
   pituitary       0.98      0.99      0.99       300

    accuracy                           0.99      1311
   macro avg       0.99      0.99      0.99      1311
weighted avg       0.99      0.99      0.99      1311
```

Pruned SqueezeNet Classification Report

```
              precision    recall  f1-score   support

      glioma       1.00      0.97      0.98       300
  meningioma       0.96      1.00      0.98       306
     notumor       1.00      1.00      1.00       405
   pituitary       0.99      0.98      0.98       300

    accuracy                           0.99      1311
   macro avg       0.99      0.99      0.99      1311
weighted avg       0.99      0.99      0.99      1311
```

Source: (Research Results, 2026)
Figure 10. Proposed Method Classification Report

Figure 10 presents the categorization reports for the suggested models: SqueezeNet Baseline and Pruned SqueezeNet. Both models attained consistently high accuracy (98,63% & 98,70%), with flawless classification noted for the notumor category. The Pruned SqueezeNet further improved recall for glioma and meningioma while maintaining balanced performance across all categories. These results confirm that pruning enhances efficiency without compromising predictive reliability, enhancing the Pruned model for optimal real-time medical application.

Models' Performance Evaluation

All evaluated models were systematically analyzed using standard performance metrics, including accuracy, precision, recall, F1-score, and AUC, which were expressed in percentage form for clearer interpretation. Stratified 5-fold cross-validation was specifically applied to the baseline and pruned SqueezeNet models to ensure a more rigorous and unbiased evaluation process. In addition, model size (KB) and inference time (ms) were measured to examine deployment feasibility, particularly for real-time medical applications where computational efficiency is critically important. Table 4 summarizes the overall performance results of all evaluated architectures.

Table 4. Models Performance Evaluation Result

No	Model	Precision (%)	Recall (%)	F1-Score (%)	Accuracy (%)	Loss
1	DenseNet121	92.72	92.52	92.46	92.52	0.1917
2	Custom CNN	94.60	94.35	94.34	94.35	0.1753
3	VGG16	84.10	84.21	83.67	84.21	0.4493
4	SqueezeNet Baseline	98.65	98.63	98.63	98.63	0.0405
5	**Proposed Pruned SqueezeNet**	**98.74**	**98.70**	**98.70**	**98.70**	**0.0438**

Source: (Research Results, 2026)

Table 4 compares the classification performance of the evaluated CNN architectures for multiclass brain tumor MRI classification. DenseNet121 and the custom CNN achieved competitive baseline performance, while VGG16 obtained lower classification accuracy and higher loss values. Both the baseline and pruned SqueezeNet models demonstrated consistently high predictive performance with low loss values.

Although the proposed pruned SqueezeNet achieved slightly higher classification accuracy than the baseline SqueezeNet, the performance difference remained relatively small. These findings suggest that the primary advantage of the pruning strategy lies in reducing computational complexity and model size while preserving competitive classification capability rather than substantially improving predictive accuracy. Table 5 summarizes the evaluation results.

Table 5. Models Efficiency

Model	Accuracy (%)	AUC Macro	Parameter (Million)	Model Size (kb)	Inference Time (ms)
VGG16	84.21	0.964	23,907,908	60,416	303.78
DenseNet 121	92.52	0.963	7,300,932	31,744	332.33
Custom CNN	94.35	0.893	22,245,700	266,240	114.41
SqueezeNet Baseline	98.63	0.997	737,476	9,011	134.38
Pruned SqueezeNet	**98.70**	**0.998**	**737,476**	**2,970**	**105.40**

Source: (Research Results, 2026)

Table 5 presents a comparison of the evaluated CNN architectures based on predictive capability and computational efficiency. DenseNet121 and VGG16 achieved relatively high classification performance; however, both architectures required significantly higher parameter counts and longer inference times

VOL. 12. NO. 1 AUGUST 2026
P-ISSN: 2685-8223 | E-ISSN: 2527-4864
DOI: 10.33480/jitk.v12i1.7963

because of their deeper network configurations. Meanwhile, the Custom CNN model produced lower inference latency, although its relatively large model size may limit its applicability in environments with restricted memory resources.

In contrast, the baseline SqueezeNet maintained high classification performance with substantially lower parameter complexity and storage requirements. Pruning was applied through weight masking rather than physical removal of filters or channels. Consequently, the reported trainable parameter count remained unchanged, while the effective sparsity, compressed model size, and inference efficiency were improved after pruning. These findings suggest that the pruning strategy effectively reduced computational redundancy without causing substantial degradation in classification performance. The ROC curve comparison of the evaluated models is presented in Figure 11.

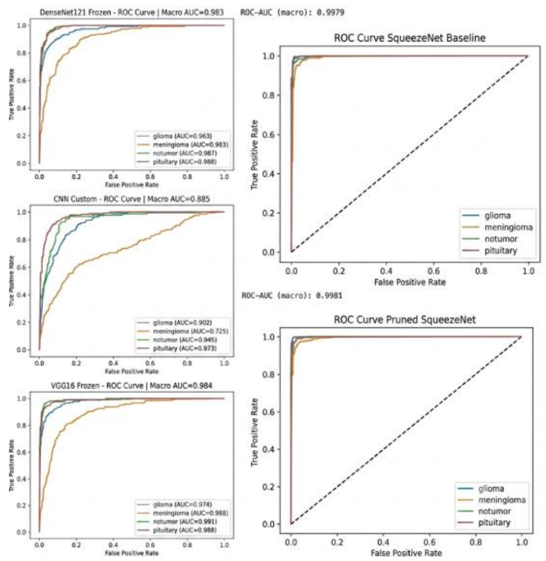

Source: (Research Results, 2026)
Figure 11. ROC Curve Comparison

Figure 11 compares the ROC curves and macro-average AUC values of the evaluated models. Both the baseline and pruned SqueezeNet achieved high AUC values, indicating strong discriminative capability across the evaluated classes. Although the proposed model obtained a slightly higher macro-average AUC, the difference relative to the baseline SqueezeNet remained marginal.

The ROC analysis indicates that the structured pruning approach maintained the model's capability to differentiate among tumor categories while simultaneously enhancing computational efficiency. The consistently high true positive rates observed across all classes also demonstrate stable and reliable classification performance for multiclass brain tumor recognition tasks.

The models accuracy comparison illustrated in Figure 12.

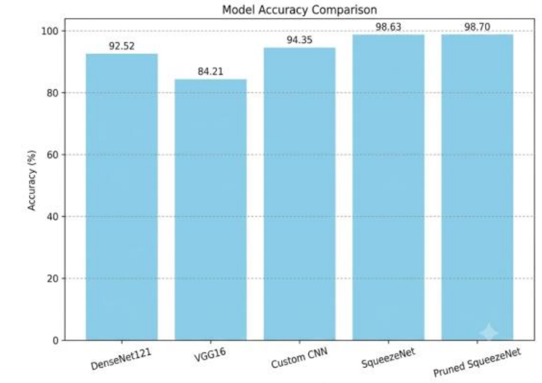

Source: (Research Results, 2026)
Figure 12. Models Accuracy Comparison

Figure 12 illustrates the classification accuracy comparison among the evaluated models. Both the baseline and pruned SqueezeNet models achieved consistently high accuracy values compared with the other CNN architectures. However, the relatively small difference between the two SqueezeNet variants indicates that the pruning strategy primarily contributed to efficiency optimization rather than substantial predictive performance improvement.

The models size comparison illustrated in Figure 13.

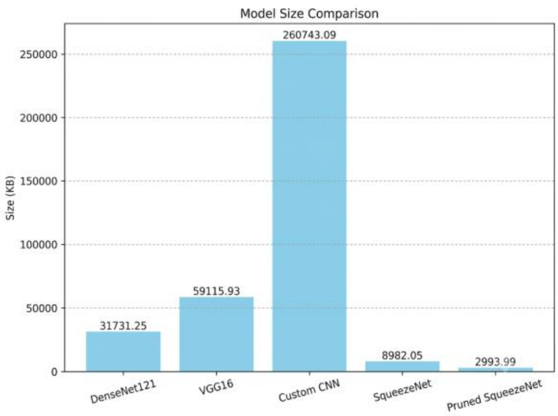

Source: (Research Results, 2026)
Figure 13. Models Size Comparison

Figure 13 highlights the differences in model storage requirements across architectures. The custom CNN exhibited the largest model size, whereas the SqueezeNet-based architectures required substantially lower storage capacity. The

VOL. 12. NO. 1 AUGUST 2026
P-ISSN: 2685-8223 | E-ISSN: 2527-4864
DOI: 10.33480/jitk.v12i1.7963

structured pruning approach further reduced model size significantly, indicating that redundant parameters could be effectively removed while preserving stable classification performance.

To further assess robustness and mitigate overfitting, stratified -fold cross-validation was conducted, with fold-wise accuracy results summarized in Table 6.

Table 6. Fold Cross-Validation Results

No	Model	Fold 1	Fold 2	Fold 3	Fold 4	Fold 5
1	SqueezeNet Baseline	98.40	98.70	98.60	98.80	98.65
2	**Proposed Pruned SqueezeNet**	**98.60**	**98.80**	**98.70**	**98.90**	**98.50**

Source: (Research Results, 2026)

Table 6 presents the cross-validation results of the baseline and proposed pruned SqueezeNet models across five validation folds. Both models demonstrated consistently high classification accuracy with only minor variations between data partitions, indicating stable predictive performance. To provide a more comprehensive statistical evaluation, the mean accuracy, standard deviation, and 95% confidence intervals were calculated and are summarized in Table 7.

Table 7. Statistical Summary Results

No	Model	Mean Accuracy (%)	Std Dev	95% CI
1	SqueezeNet Baseline	98.63	0.15	98.45 – 98.81
2	**Proposed Pruned SqueezeNet**	98.70	0.16	98.50 – 98.90

Source: (Research Results, 2026)

Table 7 indicates that both models achieved low standard deviation values across validation folds, suggesting stable classification performance. Although the proposed pruned SqueezeNet obtained slightly higher mean accuracy, the overlap between the confidence intervals indicates that the observed difference should be interpreted cautiously. These findings suggest that the pruning strategy was able to maintain competitive predictive performance while improving computational efficiency and reducing model complexity.

Comparison of baseline and Pruned SqueezeNet models with 95% confidence intervals from 5-fold cross-validation, showing stable performance and consistent improvement of the Pruned model is shown in Figure 14.

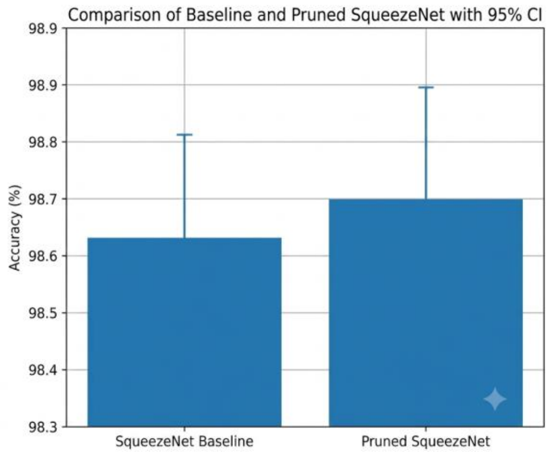

Source: (Research Results, 2026)

Figure 14. Mean Classification Accuracy with 95% Confidence Intervals Across 5-Fold Cross-Validation

Figure 14 compares the mean classification accuracy and corresponding 95% confidence intervals of the baseline and proposed pruned SqueezeNet models across stratified 5-fold cross-validation. Although the proposed model achieved slightly higher mean accuracy, the overlap between the confidence intervals indicates that the observed difference should be interpreted cautiously. The results suggest that the primary contribution of the pruning strategy lies in improving computational efficiency and reducing model complexity while maintaining competitive predictive performance.

The class-wise precision, recall, and F1-score comparison across the evaluated models indicates that both the baseline and Pruned SqueezeNet demonstrated consistently strong performance across all tumor categories, particularly for glioma and pituitary classifications. Although performance differences among the lightweight architectures were relatively small, the Pruned SqueezeNet maintained competitive class-specific performance while operating with lower computational complexity and reduced model size.

The results further suggest that the structured pruning strategy preserved essential discriminative features required for multiclass brain tumor classification. However, additional validation using more diverse MRI datasets remains necessary to evaluate model robustness under broader clinical imaging variations. The comparison of precision, recall, and F1-scores for DenseNet121, VGG16, Custom CNN, baseline SqueezeNet, and the Pruned SqueezeNet is presented in Figure 15.

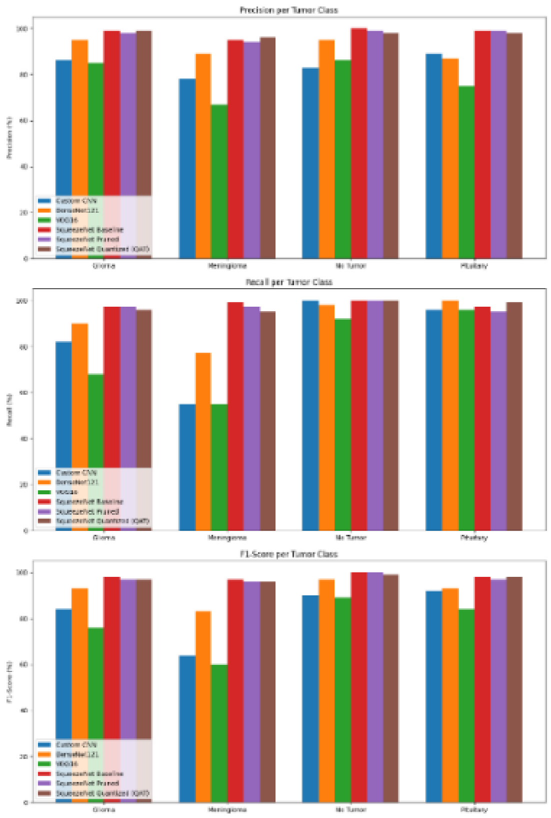

Source: (Research Results, 2026)

Figure 15. Performance Metric per Model

Furthermore, to provide a broader perspective on model efficiency and deployment feasibility, Table 8 compares the proposed Pruned SqueezeNet with previously published CNN-based approaches. The comparison highlights differences in the number of classes handled, accuracy levels, model size, and deployment focus.

Table 8 compiles recent cutting-edge studies on MRI-based brain tumor classification, which also highlights variations in model architecture, optimization techniques, and deployment viability. Overall, these findings highlight that performance improvements in deep learning models are not solely dependent on increasing model size or depth, but can also be effectively achieved through targeted parameter optimization strategies such as pruning. The proposed technique is highly apt for real-time medical imaging applications, particularly in resource-limited settings.

Despite the promising results, this study has several limitations. The experiments were conducted using a single publicly available MRI dataset, which may not fully represent variations in scanner devices, imaging protocols, and clinical acquisition conditions encountered in real-world medical environments. In addition, the proposed framework was evaluated primarily on CNN-based architectures without comparison to more recent transformer-based medical imaging models. Therefore, further validation using larger multi-institutional datasets and more diverse imaging conditions is required before broader clinical applicability can be established.

Table 8. Comparison With Related State-Of-The-Art Studies

Study	Model / Method	Classes	Dataset Size	Accuracy (%)	Model Complexity	Optimization Strategy	Deployment Suitability
Özkaraca et al., 2023 [22]	VGG16 / DenseNet (Transfer Learning)	4	Public MRI	94.00–97.00	Very High	Transfer learning	Low (heavy models)
S. Chitnis et al., 2022 [23]	Neural Architecture Search (LeaSE)	2–4	Public MRI	90.60 (AUC 95.60)	Medium–High	Neural Architecture Search (NAS)	Moderate (high search cost)
Kanchanamala et al., 2025[25]	EWHO-SqueezeNet + Hybrid Optimization	4	Public MRI	93.20	High	Metaheuristic optimization (ExpDHO + WaOA)	Limited (complex pipeline)
Sivakumar & Padmapriya, 2024 [26]	Pruned CNN	2–4	Public MRI	90.00	Medium	Weight pruning	Moderate
Ismail Oztel, 2025 [24]	Ensemble CNN + Vision Transformer	4	Public MRI	85.53	High	Wavelet Transform + Bagging Ensemble	Low-Moderate
Proposed Method	**Structured Pruned SqueezeNet**	**4**	**7,023 MRI**	**98.70**	**Low**	**Structured pruning (Polynomial Decay)**	**High (real-time, edge-ready)**

Source: (Research Results, 2026)

VOL. 12. NO. 1 AUGUST 2026
P-ISSN: 2685-8223 | E-ISSN: 2527-4864
DOI: 10.33480/jitk.v12i1.7963

CONCLUSION

This study investigated multiple deep learning architectures for multiclass brain tumor MRI classification, including VGG16, DenseNet121, Custom CNN, baseline SqueezeNet, and the proposed pruned SqueezeNet model. Experimental findings demonstrated that deeper architectures such as DenseNet121 produced strong classification performance; however, their high parameter complexity and extended inference times may reduce suitability for deployment in computationally limited environments. To overcome these challenges, this research introduced a structured pruning approach combined with polynomial decay sparsity scheduling on the lightweight SqueezeNet architecture. The proposed framework achieved a classification accuracy of 98.70% with an inference time of 105.40 ms while reducing the model size to approximately 2,993 KB and improving computational efficiency. These results indicate that structured pruning can effectively minimize computational redundancy while retaining the important discriminative features required for multiclass brain tumor classification. Although the proposed pruned model produced slightly better predictive performance compared with the baseline SqueezeNet architecture, the performance improvement itself was relatively limited. Therefore, the main contribution of this study lies in enhancing computational efficiency, minimizing storage requirements, and reducing inference time while maintaining competitive classification capability. Despite these promising outcomes, several limitations remain in this study. The experiments relied on a single publicly available MRI dataset, which may not fully capture variations in scanner devices, institutional imaging protocols, and real-world clinical acquisition conditions. Furthermore, the investigation primarily focused on CNN-based architectures without extensive comparison against more recent transformer-based medical imaging approaches. Consequently, additional validation using larger and more diverse multi-institutional MRI datasets is still required before broader clinical implementation can be considered. Future research will focus on improving model robustness and interpretability through robustness evaluation under varying imaging conditions, noise perturbations, and MRI acquisition settings. Explainable artificial intelligence methods such as Grad-CAM may also be integrated to provide visual interpretation of prediction results. In addition, further compression techniques, including post-training quantization and quantization-aware training, will be explored to support efficient deployment on embedded and edge-based healthcare systems.

REFERENCE

[1] R. Preetha, M. J. P. Priyadarsini, and J. S. Nisha, “Automated Brain Tumor Detection From Magnetic Resonance Images Using Fine-Tuned EfficientNet-B4 Convolutional Neural Network,” *IEEE Access*, vol. 12, no. July, pp. 112181–112195, 2024, doi: 10.1109/ACCESS.2024.3442979.

[2] W. Chen, P. Sun, and Y. Zhang, “A brain tumor diagnosis approach based on deep separable convolutional networks and attention mechanisms,” *Appl. Comput. Eng.*, vol. 67, no. 1, pp. 60–69, Jul. 2024, doi: 10.54254/2755-2721/67/20240629.

[3] J. Kang, Z. Ullah, and J. Gwak, “MRI-Based Brain Tumor Classification Using Ensemble of Deep Features and Machine Learning Classifiers,” *Sensors*, vol. 21, no. 2222, pp. 1–21, Mar. 2021, doi: 10.3390/s21062222.

[4] Y. E. Almalki *et al.*, “Isolated Convolutional-Neural-Network-Based Deep-Feature Extraction for Brain Tumor Classification Using Shallow Classifier,” *Diagnostics*, vol. 12, no. 8, p. 1793, Jul. 2022, doi: 10.3390/diagnostics12081793.

[5] M. Aamir *et al.*, “Brain Tumor Detection and Classification Using an Optimized Convolutional Neural Network,” *Diagnostics*, vol. 14, no. 1714, pp. 1–19, Aug. 2024, doi: 10.3390/diagnostics14161714.

[6] I. Pacal, O. Celik, B. Bayram, and A. Cunha, “Enhancing EfficientNetv2 with global and efficient channel attention mechanisms for accurate MRI-Based brain tumor classification,” *Cluster Comput.*, vol. 27, no. 8, pp. 11187–11212, Nov. 2024, doi: 10.1007/s10586-024-04532-1.

[7] N. Zheng, G. Zhang, Y. Zhang, and F. R. Sheykhahmad, “Brain tumor diagnosis based on Zernike moments and support vector machine optimized by chaotic arithmetic optimization algorithm,” *Biomedical Signal Processing and Control*, vol. 82, p. 104543, Apr. 2023, doi: 10.1016/j.bspc.2022.104543.1

[8] M. A. Purnama Wibowo, Muhammad Bima Al Fayyadl, Yufis Azhar, and Zamah Sari,

"Classification of Brain Tumors on MRI Images Using Convolutional Neural Network Model EfficientNet," *J. RESTI (Rekayasa Sist. dan Teknol. Informasi)*, vol. 6, no. 4, pp. 538–547, Aug. 2022, doi: 10.29207/resti.v6i4.4119.

[9] S. Agarwal, D. Jain, S. Gupta, S. Sawhney, and Y. Mittal, "Brain Tumor Detection and Classification Using Deep Learning," in *2023 5th International Conference on Advances in Computing, Communication Control and Networking (ICAC3N)*, 2023, pp. 635–640. doi: 10.1109/ICAC3N60023.2023.10541584.

[10] A. B. Abdusalomov, M. Mukhiddinov, and T. K. Whangbo, "Brain Tumor Detection Based on Deep Learning Approaches and Magnetic Resonance Imaging," *Cancers (Basel).*, vol. 15, no. 4172, pp. 1–29, Aug. 2023, doi: 10.3390/cancers15164172.

[11] M. T. C. Seng and N. H. bt Rashidi, "Enhanced Brain Tumor Classification using Modified ResNet50 Architecture," *Borneo J. Sci. Technol.*, vol. 6, no. 1, pp. 11–18, Jan. 2024, doi: 10.35370/bjost.2024.6.1-02.

[12] Q. T. Lu, T. M. Nguyen, and H. Le Lam, "Improving Brain Tumor MRI Image Classification Prediction based on Fine-tuned MobileNet," *Int. J. Adv. Comput. Sci. Appl.*, vol. 15, no. 1, pp. 540–550, 2024, doi: 10.14569/IJACSA.2024.0150152.

[13] A. Agrawal, "Classification and Detection of Brain Tumors by Aquila Optimizer Hybrid Deep Learning Based Latent Features with Extreme Learner," *ITM Web Conf.*, no. 02008, p. 02008, Jun. 2023, doi: 10.1051/itmconf/20235302008.

[14] N. Elazab, W. Gab Allah, and M. Elmogy, "Computer-aided diagnosis system for grading brain tumor using histopathology images based on color and texture features," *BMC Med. Imaging*, vol. 24, no. 1, pp. 1–22, 2024, doi: 10.1186/s12880-024-01355-9.

[15] I. Akbari, D. Hartama, and A. Wanto, "OPTIMIZATION OF EFFICIENTNET-B0 ARCHITECTURE TO IMPROVE THE ACCURACY OF GLAUCOMA DISEASE CLASSIFICATION," *JITK (Jurnal Ilmu Pengetah. dan Teknol. Komputer)*, vol. 11, no. 2, pp. 342–352, Nov. 2025, doi: 10.33480/jitk.v11i2.7140.

[16] M. Güler and E. Namlı, "Brain Tumor Detection with Deep Learning Methods' Classifier Optimization Using Medical Images," *Appl. Sci.*, vol. 14, no. 642, pp. 1–25, Jan. 2024, doi: 10.3390/app14020642.

[17] P. K. Ramtekkar, A. Pandey, and M. K. Pawar, "Accurate detection of brain tumor using optimized feature selection based on deep learning techniques," *Multimed. Tools Appl.*, vol. 82, no. 29, pp. 44623–44653, Dec. 2023, doi: 10.1007/s11042-023-15239-7.

[18] A. Z. Al Wafi, F. P. Rochim, and A. Fathimah, "Deep Learning Approach for Pneumonia Prediction from X-Rays using A Pretrained Densenet Model," *J. ELTIKOM*, vol. 9, no. 1, pp. 98–106, Jun. 2025, doi: 10.31961/eltikom.v9i1.1457.

[19] Solikhun, A. P. Windarto, and P. Alkhairi, "Bone fracture classification using convolutional neural network architecture for high-accuracy image classification," *Int. J. Electr. Comput. Eng.*, vol. 14, no. 6, pp. 6466–6477, 2024, doi: 10.11591/ijece.v14i6.pp6466-6477.

[20] A. I. R. H. Barat, W. S. Astuti, D. Hartama, A. P. Windarto, and A. Wanto, "ENHANCED FLOWER IMAGE CLASSIFICATION USING MOBILENETV2 WITH OPTIMIZED PERFORMANCE," *JITK (Jurnal Ilmu Pengetah. dan Teknol. Komputer)*, vol. 11, no. 1, pp. 180–191, Aug. 2025, doi: 10.33480/jitk.v11i1.6497.

[21] M. O. Khairandish, M. Sharma, V. Jain, J. M. Chatterjee, and N. Z. Jhanjhi, "A Hybrid CNN-SVM Threshold Segmentation Approach for Tumor Detection and Classification of MRI Brain Images," *Irbm*, vol. 43, no. 4, pp. 290–299, 2022, doi: 10.1016/j.irbm.2021.06.003.

[22] O. Özkaraca *et al.*, "Multiple Brain Tumor Classification with Dense CNN Architecture Using Brain MRI Images," *Life*, vol. 13, no. 2, p. 349, Jan. 2023, doi: 10.3390/life13020349.

[23] S. Chitnis, R. Hosseini, and P. Xie, "Brain tumor classification based on neural architecture search," *Sci. Rep.*, vol. 12, no. 1, p. 19206, Nov. 2022, doi: 10.1038/s41598-022-22172-6.

[24] I. Oztel, "Ensemble Deep Learning Approach for Brain Tumor Classi fi cation Using Vision Transformer and Convolutional Neural Network," vol. 2500393, pp. 1–10, 2025, doi: 10.1002/aisy.202500393.

[25] P. Kanchanamala, R. Karnati, and R. K. Tammineni, "Brain tumor classification from MRI images using exponential-Walruses hunting optimization driven SqueezeNet," *Expert Syst. Appl.*, vol. 271, no. 5, p. 126633, May 2025, doi: 10.1016/j.eswa.2025.126633.

VOL. 12. NO. 1 AUGUST 2026
P-ISSN: 2685-8223 | E-ISSN: 2527-4864
DOI: 10.33480/jitk.v12i1.7963

[26] M. Sivakumar and S. T. Padmapriya, “Improving Efficiency of Brain Tumor Classification Models Using Pruning Techniques,” *Curr. Med. Imaging Former. Curr. Med. Imaging Rev.*, vol. 20, pp. 1–12, Aug. 2024, doi: 10.2174/0115734056303076240614113525.

[27] K. R. Reddy and R. Dhuli, “A Novel Lightweight CNN Architecture for the Diagnosis of Brain Tumors Using MR Images,” *Diagnostics*, vol. 13, no. 312, pp. 1–21, Jan. 2023, doi: 10.3390/diagnostics13020312.

[28] M. Rasool, N. A. Ismail, A. Al-Dhaqm, W. M. S. Yafooz, and A. Alsaeedi, “A Novel Approach for Classifying Brain Tumours Combining a SqueezeNet Model with SVM and Fine-Tuning,” *Electron.*, vol. 12, no. 1, 2023, doi: 10.3390/electronics12010149.

[29] L. Li, Y. Kong, and Q. Zhang, “Lightweight Malicious Code Classification Method Based on Improved SqueezeNet,” *Comput. Mater. Contin.*, vol. 78, no. 1, pp. 551–567, 2024, doi: 10.32604/cmc.2023.045512.

[30] L. Narayanan, “A Hybrid Deep Learning Based Assist System for Detection and Classification of Breast Cancer from Mammogram Images,” *Int. Arab J. Inf. Technol.*, vol. 19, no. 6, pp. 965–974, 2022, doi: 10.34028/iajit/19/6/15.

[31] A. Bin Naeem *et al.*, “Lightweight CNN for accurate brain tumor detection from MRI with limited training data,” *Frontiers in Medicine*, vol. 12, Aug. 2025, doi: 10.3389/fmed.2025.1636059.

[32] M. Zabin, A. N. Binte Kabir, M. K. Kabir, H. J. Choi, and J. Uddin, “Machine Fault Diagnosis Using EMD-Gammatone Texture Representation and A Lightweight Self-Attention SqueezeNet,” *2024 IEEE International Conference on Big Data and Smart Computing (BigComp)*, pp. 32–39, Feb. 2024, doi: 10.1109/bigcomp60711.2024.00015.

[33] C. Xie *et al.*, “A Novel Fusion Pruning-Processed Lightweight CNN for Local Object Recognition on Resource-Constrained Devices,” *IEEE Trans. Consum. Electron.*, vol. 70, no. 4, pp. 6713–6724, Nov. 2024, doi: 10.1109/TCE.2024.3475517.

[34] M. Hao, Q. Sun, C. Xuan, X. Zhang, and M. Zhao, “SqueezeNet: An Improved Lightweight Neural Network for Sheep Facial Recognition,” *Appl. Sci.*, vol. 14, no. 4, pp. 1–13, Feb. 2024, doi: 10.3390/app14041399.

[35] J. Tmamna, E. Ben Ayed, R. Fourati, A. Hussain, and M. Ben Ayed, “A CNN pruning approach using constrained binary particle swarm optimization with a reduced search space for image classification,” *Appl. Soft Comput.*, vol. 164, p. 111978, Oct. 2024, doi: 10.1016/j.asoc.2024.111978.

[36] M. Xia, Z. Zhong, and D. Chen, “Structured Pruning Learns Compact and Accurate Models,” *Proceedings of the 60th Annual Meeting of the Association for Computational Linguistics (Volume 1: Long Papers)*, pp. 1513–1528, 2022, doi: 10.18653/v1/2022.acl-long.107.

[37] M. Nickparvar, *Brain Tumor*. 2021. [Online]. Available: https://www.kaggle.com/datasets/masoudnickparvar/brain-tumor-mri-dataset

[38] K. N. A. Nur, A. Wanto, and P. Poningsih, “OPTIMIZATION OF SVM ALGORITHM FOR OBESITY CLASSIFICATION WITH SMOTE TECHNIQUE AND HYPERPARAMETER TUNING,” *JITK (Jurnal Ilmu Pengetahuan dan Teknologi Komputer)*, vol. 11, no. 2, pp. 291–303, Nov. 2025, doi: 10.33480/jitk.v11i2.6878.

[39] O. Nurdiawan, H. Susana, and A. Faqih, “Deep Learning for Polycystic Ovarian Syndrome Classification Using Convolutional Neural Network,” *JITK (Jurnal Ilmu Pengetah. dan Teknol. Komputer)*, vol. 9, no. 2, pp. 218–226, 2024, doi: 10.33480/jitk.v9i2.4575.

[40] S. Makenali, B. Rokh, and A. Azarpeyvand, "Integrating Pruning with Quantization for Efficient Deep Neural Networks Compression," *arXiv preprint* arXiv:2509.04244, 2025. [Online]. Available: https://arxiv.org/abs/2509.04244.